Journal of Structural Geology, Vol. 13, No. 3, pp. 349 to 356, 1991
Printed in Great Britain

0191-8141/91 $03.00+0.00
Pergamon Press plc

Rotation, offset and separation of oblique-fracture (rhombic) boudins: theory and experiments under layer-normal compression

NIBIR MANDAL and DEBDARPAN KHAN

Department of Geological Sciences, Jadavpur University, Calcutta-700 032, India

(*Received* 3 *October* 1989; *accepted in revised form* 3 *June* 1990)

Abstract—Boudinage structures are generally produced by extension fracturing of competent rocks normal to layering. Boudin-like structures may also develop by shear fracturing of competent rocks oblique to layering. In such structures boudins of rhomboid shape are rotated and offset with respect to each other. It is usually considered that shear fracture boudins do not get separated until a critical rotation is attained, when they can just touch each other. However, the experiments under layer-normal compression and the theoretical analysis of the present study indicate that the layer-segments produced by a set of parallel shear fractures may undergo rotation with separation or rotation with interfacial slip depending upon their geometry. The thickness to length ratio (G_r) of layer-segments and the orientation of fractures (ϕ) are the parameters that could control the rate of rotation versus rate of displacement of layer-segments.

INTRODUCTION

BOUDINAGE structure is one of the characteristic features of rocks that have layers of contrasting competency and have undergone layer-parallel extension. The classical type of boudinage structures, as described by Lohest (1909), Corin (1932), Wegmann (1932) and Ramberg (1955), develop due to extension-fracturing of competent layers perpendicular to the layering. Such boudinaged layers show separated rectangular segments and the separation zones are generally filled with vein-materials. Boudin-like structures in competent layers may also develop by shear fracturing (Cloos 1947, Uemura 1965). In this type of boudinage, competent layers are offset by layer-oblique shear fractures producing a series of faulted rhomboid blocks in a ductile matrix (e.g. fig. 2.16 of Ramsay & Huber 1983).

Shear fractures, associated with boudinage structures, were obtained in rock deformation experiments by Griggs & Handin (1960), Paterson & Weiss (1968) and Gay & Jaeger (1975). Tvergaard *et al.* (1981) have also shown from finite element analysis that several types of shear bands may develop in a layer depending upon the rheological property and the initial geometrical inhomogeneities. Experimental models consisting of rigid layers, segmented by parallel oblique-cuts, and embedded in viscous media show rotation and offset of the layer-segments in response to layer-normal compression (Karmakar & Mandal 1989). The sense of rotation and offset of the segments are consistent with overall extension of the layers.

It is generally considered that during layer-parallel extension of a competent layer, segmented by a series of parallel shear fractures, the individual layer-segments start to rotate about their centres. The rotation is accompanied by slip along the fractures causing offset, and the segments do not get separated until a critical rotation is attained when the layer segments can just touch each other (Fig. 1a). However, in many natural deformed rocks (fig. 118b of Stach 1982, Ramsay & Huber 1987, p. 633) rigid rhombic boudins are observed to have been separated from each other before the critical rotation of boudins was reached (Fig. 1b). This fact suggests that in certain situations, separation of layer-segments may accompany rotation of the segments following initiation of shear fractures.

In this paper we use theory and experiments to analyse the mode of displacement of layer-segments, separated by oblique fractures, of a rigid layer embedded in a ductile matrix under layer-normal compression. Our

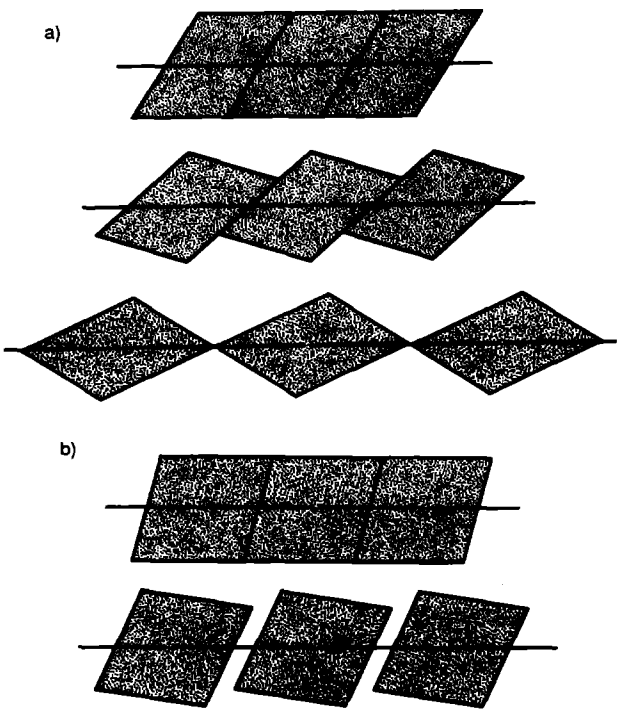

Fig. 1. Schematic diagram showing (a) critical stage of rotation of layer-segments just prior to separation in the evolution of typical shear fracture boudinage and (b) boudinage structure rendered through simultaneous separation and rotation of layer-segments.

theoretical analysis considers displacement of the layer-segments as a response to the layer-parallel viscous flow of the surrounding matrix and we derive a mathematical equation involving parameters in relation to geometry of layer-segments and orientation of fractures. The graphical representation of the equation reveals two fields in a co-ordinate system of the two parameters mentioned above. In one of the fields layer-segments would show rotation and offset without producing any separation; in the other the segments would not be in contact with each other immediately after initiation of fractures, and would separate along with their rotation. Our experimental observations concur with the theoretical results.

EXPERIMENTS ON ROTATION AND SEPARATION OF BOUDINS

A rigid wax layer, segmented by a series of cuts oblique to the layering, was submerged in a block of pitch (viscous medium). The top of the wax layer was at the same level as the top of the pitch. The pitch-block was sided by two wooden bars parallel to the wax layer (Fig. 2). The interfaces between the pitch and the wooden bars were smeared with soapy-water to lubricate the flow of pitch along these surfaces. The model was set on a glass plate that was smeared with the same lubricant to minimize friction to viscous flow at the bottom. The pitch-block was shortened by moving the wooden bars towards each other in the direction perpendicular to the layering. During the deformation, a glass plate was pressed over the model to restrict swelling of the pitch in the vertical direction.

With the help of this model set-up, a number of experiments were carried out using rigid layers of different width to length ratio (G_r) of layer-segments and different angles of cut (ϕ) with the layer-normal. The experimental results are summarized below.

(a) *Experiment with* $G_r = 0.5$ *and* $\phi = 30°$

Under layer-normal compression the model showed development of separation zones accompanying rotation of the layer-segments (Fig. 3a). However, the angular changes of the layer-segments due to rotation were small compared to the width of the separation zones which increased significantly during progressive deformation of the model (Fig. 3ai–iii).

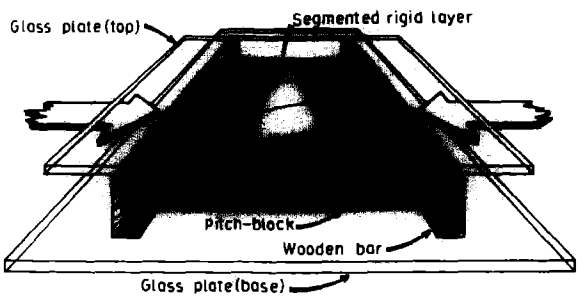

Fig. 2. A schematic sketch of the experimental set-up.

(b) *Experiment with* $G_r = 2.0$ *and* $\phi = 28°$

In this experiment (Fig. 3b) no separation zones were produced at any stage of deformation of the model. The layer was offset by rotation of the layer-segments producing structures which looked very similar to typical shear fracture boudinage structure (Ramsay & Huber 1983). The magnitude of offset increased with increase in rotation of the layer-segments during progressive deformation of the model.

(c) *Experiment with* $G_r = 1.0$ *and* $\phi = 26°$

Separation zones were again obtained accompanying rotation of the layer-segments similar to that in experiment (a). However, the width of the separation zones did not increase at a comparable rate to that in experiment (a). A comparison of the two experiments reveals that the layer-segments of this experiment (c) underwent a greater amount of rotation for a unit increment of separation (Fig. 3c).

A set of experiments was done to reveal the nature of displacement of layer-segments when fractures are at a high angle to the layer-normal. The rigid wax layer has oblique cuts at an angle of 45° with the layering. The experiments were conducted with different values of G_r with an aim to understanding how the variation of width to length ratio of layer-segments could affect the development of boudinage structures for a fixed value of ϕ. The experimental results are summarized below.

(d) *Experiment with* $\phi = 45°$ *and* $G_r = 0.85$

Under layer-normal compression the rigid layer underwent rotation and offset of the layer-segments (Fig. 4a). Separation zones were not produced at any stage of progressive deformation of the model (Fig. 4ai–iii).

(e) *Experiment with* $\phi = 45°$ *and* $G_r = 0.6$

The experiment exhibited a similar structural evolution (Fig. 4b) to that shown by experiment (d). However, the rotation and hence offset of the layer-segments did not increase at the same rate in the two experiments (Fig. 4bi–iii).

(f) *Experiment with* $\phi = 45°$ *and* $G_r = 0.2$

At this value of G_r separation zones along with rotation of the layer-segments were obtained (Fig. 4c). The amount of rotation of the segments increased with separation but not at the rate shown by the previous two experiments (Fig. 4ci–iii).

THEORETICAL ANALYSIS

Let ABCD and EFBA be the cross-sections of any two adjacent segments of a rigid, segmented layer in an

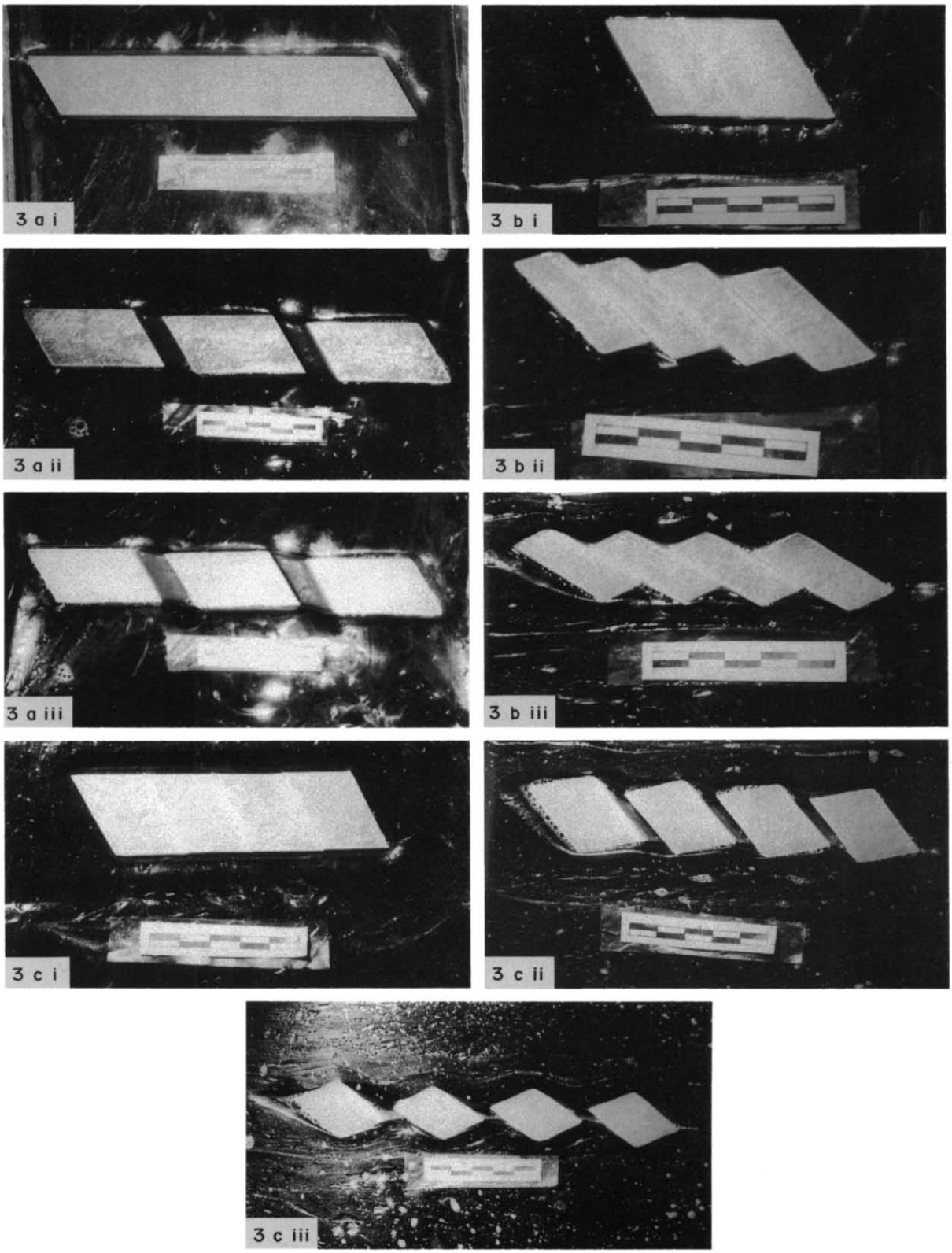

Fig. 3. Successive stages of development of boudinage structures in segmented layers for (a) $G_r = 0.5$ and $\phi = 30°$, (b) $G_r = 2.0$ and $\phi = 28°$ and (c) $G_r = 1.0$ and $\phi = 26°$. (i), (ii) and (iii) are three stages of each experiments. Note that in (c) separation to rotation ratio is lower than that in (a).

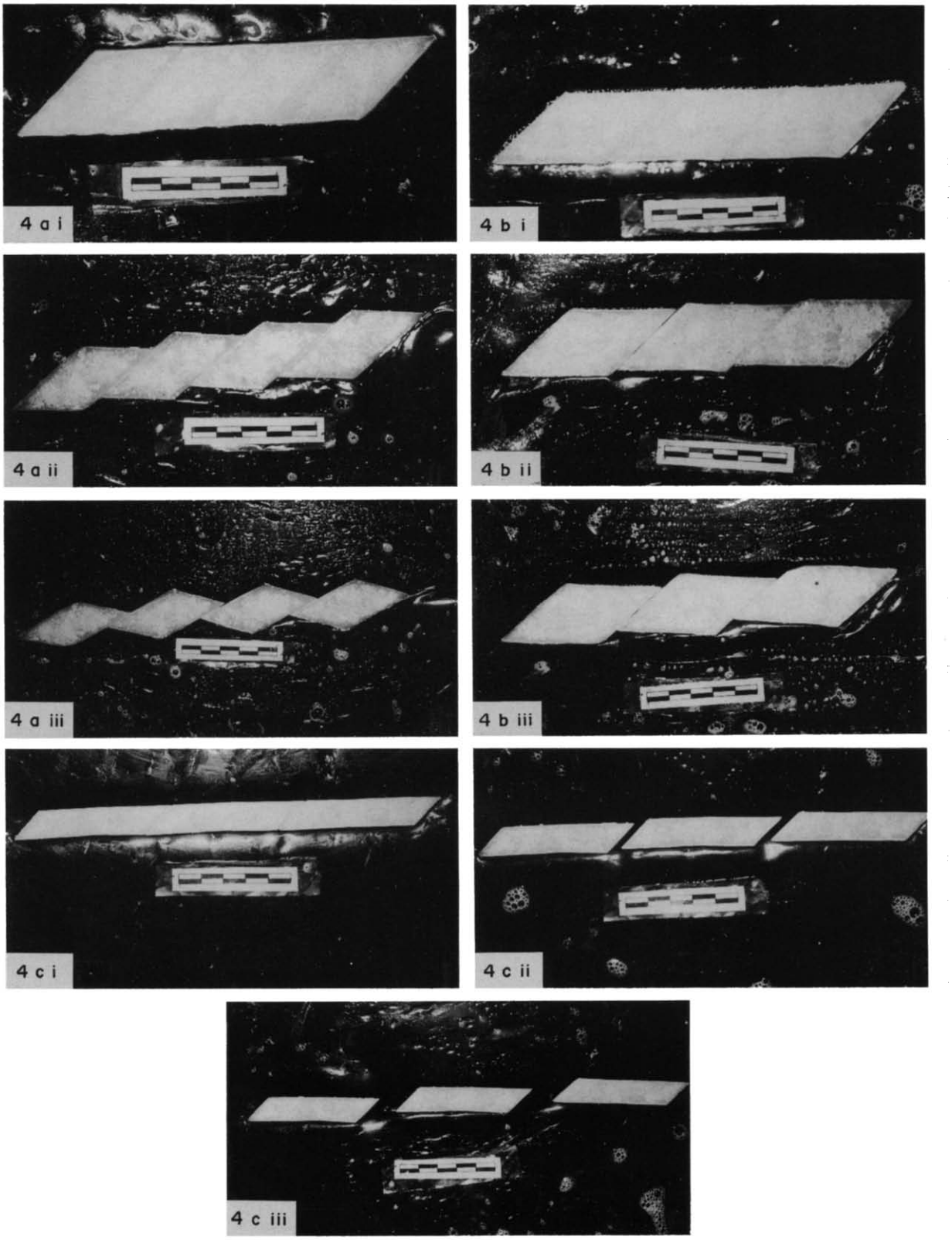

Fig. 4. Successive stages of boudinage structures in segmented layers with $\phi = 45°$ and $G_r = 0.85$, 0.6 and 0.2 in (a), (b) & (c), respectively. (i), (ii) and (iii) are the three stages of each experiment. Note that in (b) rotation of the layer-segments is smaller than that in (a).

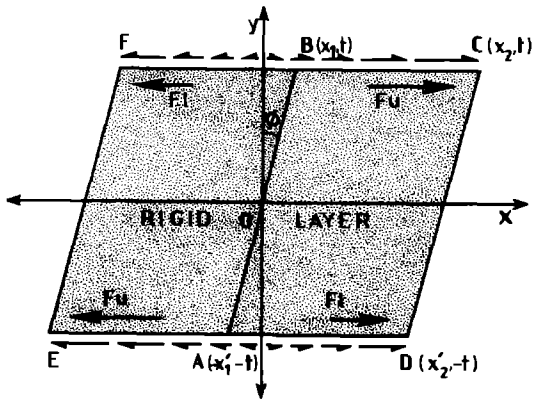

Fig. 5. Geometrical representation of two adjacent segments of a layer in a co-ordinate frame x, y; the arrows on the boundaries and inside the boundaries indicate shear stresses exerted by a viscous flow and the resultant forces on the segments, respectively.

infinitely extended viscous medium (Fig. 5). Under a layer-normal compression the viscous flow of the matrix exerts shear stresses over the layer-surfaces, and results in displacement of the segments. Let F_u and F_l be the forces on the faces BC and AD, respectively. In the assumed frame of reference (x, y) the magnitude of forces on the upper and lower faces of the segment EFBA correspond to that on the lower and upper faces of the segment ABCD, respectively. It is apparent from Fig. 5 that F_u and F_l are unequal in magnitude (in this case $F_u > F_l$). Since F_u is greater than F_l, the amount by which F_u exceeds F_l would act as a coupling force on the segment; whereas the amount of F_u that equals F_l along with the force F_l would act as a translatory force. Thus, the coupling force $F_R = F_u - F_l$ would tend to rotate the segments and the force $2F_l$ would tend to pull apart the segments from each other. The forces F_u and F_l can be written in terms of a stress function as

$$F_u = \int_{x_1}^{x_2} \tau(x)\,dx \tag{1a}$$

$$F_l = \int_0^{x_2'} \tau(x)\,dx + \int_0^{-x_1'} \tau(x)\,dx, \tag{1b}$$

where $\tau(x)$ is the shear stress function on the rigid layer for viscous flow; x_1, x_2, $-x_2'$ are the abscissae of the corners of the segment ABCD which can be given as

$$x_1 = t + \tan\phi \tag{2a}$$

$$x_2 = d + \tan\phi \tag{2b}$$

$$x_1' = t\tan\phi \tag{2c}$$

$$x_2' = d - t\tan\phi, \tag{2d}$$

where $2t$ and d are the layer-thickness and the length of the layer-segments, and ϕ is the angle between fractures and the layer-normal (Fig. 5).

Stress function

Let us choose a reference frame (X, Y) where the Y axis is perpendicular to the layer and the X axis coincides with the surface of the rigid layer and is parallel to the bulk extension. This is related to the previous reference frame as $Y = y - t$ and $X = x$. In the region far away from the rigid surface the stream function of a viscous flow can be given as

$$\psi = aXY, \tag{3}$$

where a is a constant which can be solved as

$$a = \frac{\partial^2\psi}{\partial X\partial Y}$$

$$\frac{\partial U}{\partial X} = \dot{e}_X^*, \tag{4}$$

where $\dot{e}_X^*$ is the far-field strain rate along the X axis of the viscous medium.

However, the stream function in the neighbourhood of the rigid layer will be different from that of the far-field region because of the restriction of the viscous flow on the rigid surfaces. Since the velocity-component along the Y axis is independent of X, i.e. a material line parallel to the rigid layer remains in the same orientation during deformation, the differential form of the general stream function in the neighbourhood of the rigid surfaces can be expressed as

$$\frac{\partial\psi}{\partial X} = \varphi(Y) + \varphi_0(Y), \tag{5}$$

where $\varphi_0(Y)$ stands for the differential form of the far-field stream function, given in equation (4), with respect to X. $\varphi(Y)$ is the additional function imposed by the flow-restriction at the surface which will satisfy the following boundary conditions:

$$\varphi(Y) \to 0 \quad \text{as} \quad Y \to \infty \quad \text{and} \quad 0. \tag{6}$$

To satisfy the above boundary conditions $\varphi(Y)$ can be expressed as

$$\varphi(Y) = CYe^{-KY}, \tag{7}$$

where C and K are constants. Then, the general stream function becomes

$$\frac{\partial\psi}{\partial X} = CYe^{-KY} + \dot{e}_X^* Y. \tag{8}$$

The solution of the above equation gives

$$\psi = (Ce^{-KY} + \dot{e}_X^*)XY + \text{constant}. \tag{9}$$

The velocity-component along the X axis at a point in the neighbourhood of the rigid surfaces can be obtained by differentiating equation (9) with respect to Y as

$$U = (Ce^{-KY} - CKe^{-KY} + \dot{e}_X^*)X. \tag{10}$$

Imposing the boundary condition $U = 0$ at $Y = 0$ in equation (10) we get $C = -\dot{e}_X^*$. Then equation (9) can be written as

$$\psi = \dot{e}_X^*(1 - e^{-KY})XY + \text{constant}. \tag{11}$$

The velocity-gradient of U in the direction of the Y axis at any point in the neighbourhood of the rigid

surface can be obtained by taking the second-order derivative of equation (11) with respect to Y as

$$\frac{\partial U}{\partial Y} = K\dot{e}_X^*(2e^{-KY} - KYe^{-KY})X. \tag{12}$$

At the rigid surface $Y = 0$

$$\left(\frac{\partial U}{\partial Y}\right)_{Y=0} = 2K\dot{e}_X^* X. \tag{13}$$

The shear stresses on the rigid surface exerted by a viscous flow at any point $(X, 0)$ can be solved with the help of equation (13) as

$$\tau(X) = \eta\left(\frac{\partial U}{\partial Y}\right)_{Y=0} = 2K\eta\dot{e}_X^* X, \tag{14}$$

where η is the coefficient of viscosity of the embedding medium. Now the stress function on the boundary of the rigid layer can be transformed to xy co-ordinates as

$$\tau(x) = 2\eta K\dot{e}_x^* x. \tag{15}$$

Forces on segments of the rigid layer

Forces F_u and F_l on the segment ABCD can be evaluated by substituting the expression of stress function from equation (15) in equation (1). Then we get

$$F_u = \int_{x_1}^{x_2} 2\eta K\dot{e}_x^* \,dx = \eta K\dot{e}_x^*(x_2^2 - x_1^2). \tag{16}$$

Substituting the values of x_1 and x_2 from equations (2a) and (2b) in equation (1) F_u can be rewritten after simplification as

$$F_u = \eta K\dot{e}_x^*(d^2 + 2dt\tan\phi). \tag{16a}$$

Similarly F_l can be solved with the help of equations (1b) and (15) and after simplification it can be written as

$$F_l = \eta K\dot{e}_x^*(d^2 - 2dt\tan\phi). \tag{17}$$

The layer-segments will tend to be pulled apart from each other by a force

$$F_D = 2F_l = 2\eta K\dot{e}_x^*(d^2 - 2dt\tan\phi) \tag{18}$$

and the coupling component of the forces F_u and F_l which tend to rotate each segments will be given by

$$F_R = F_u - F_l = 4\eta K\dot{e}_x^* dt\tan\phi. \tag{19}$$

Separation vs rotation of layer-segments

In order to understand separation vs rotation of boudins the rates of displacements of centres of the segments under a pulling force F_D and under a coupling force F_R may be analysed separately and then considered together for mathematical convenience.

(i) *Displacement of layer-segments under a pulling force* F_D. Under a translation motion, a material line perpendicular to layering and stuck to the surface of a layer-segment will be deflected and the deflection will die out asymptotically away from the rigid layer. The deflected configuration of the material line for unit time representing variation of velocity-component along the x axis in the neighbourhood of the moving layer-segments can be expressed as

$$\dot{X} = \tfrac{1}{2}\dot{D}e^{-Y}, \tag{20a}$$

where $\dot{D}$ is the rate of displacement of one layer-segment with respect to its adjacent layer-segment. By differentiating equation (20a) we get

$$\frac{d\dot{X}}{dY} = -\frac{1}{2}\dot{D}e^{-Y}$$

and at $Y = 0$

$$\frac{d\dot{X}}{dY} = -\frac{1}{2}\dot{D}. \tag{20b}$$

Drag force per unit area can be evaluated from the velocity gradient at the boundary of the layer-segments given in equation (20b), and is given by

$$\tau = \eta\frac{d\dot{X}}{dY} = -\frac{1}{2}\eta\dot{D}. \tag{21}$$

By equating the magnitude of the pulling force given in equation (18) and the drag force given in equation (21) on a segment we get

$$\dot{D} = 2\dot{e}_x^* K(d - 2t\tan\phi). \tag{22}$$

(ii) *Displacement of layer-segments due to rotation.* Let the co-ordinates of one of the corners of a segment be (x, y) (Fig. 6), where

$$x = r\cos\theta - \tfrac{1}{2}d \quad \text{and} \quad y = r\sin\theta.$$

Differentiating with respect to time

$$\frac{dx}{dt} = -r\sin\theta\frac{d\theta}{dt}$$

or

$$\dot{S}_x = \frac{dx}{dt} = -y\dot{W}, \tag{23}$$

where $\dot{S}_x$ is the rate of displacement-component of the point along the x axis for a rate of rotation $\dot{W}$ which can be equated with the force along x axis in a similar way to the previous case. Then we get

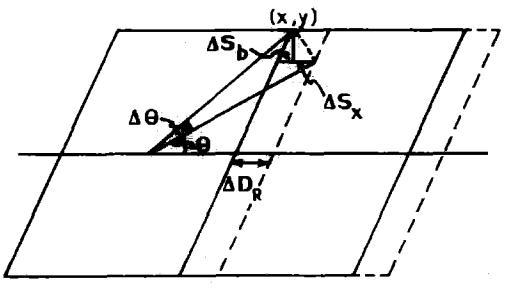

Fig. 6. Diagram showing displacement-components of a layer-segment due to its rotation.

$$\dot{S}_x = 2\dot{e}_x^* t \tan\phi. \quad (24)$$

Again,

$$y = r\sin\theta$$

or

$$dy = \cos\theta\, d\theta$$

or

$$dy = (\tfrac{1}{2}d + t\tan\phi)\, d\theta. \quad (25a)$$

From Fig. 6

$$dS_b = (\tfrac{1}{2}d + t\tan\phi)\tan\theta\, d\theta. \quad (25b)$$

Then the total displacement of centres of the segments in the x-direction required to accommodate a small amount of rotation $d\theta$ (Fig. 6) can be written as

$$dD_R = dS_x + dS_b$$

or

$$dD_R = (t\sec^2\phi + \tfrac{1}{2}d\tan\phi)\, d\theta. \quad (26a)$$

With the help of equations (23) and (24) equation (26a) can be modified to

$$\dot{D}_R = 2K\dot{e}_x^*(t\sec^2\phi + \tfrac{1}{2}d\tan\phi)\tan\phi. \quad (26b)$$

$\dot{D}_R$ is the rate of displacement of centres of the segments consequential to rotation.

(iii) *Separation vs rotation-and-offset of layer-segments.* Now the ratio of the two rates $\dot{D}$ and $\dot{D}_R$ may be used to envisage the influence of the geometry of layer-segments on the processes of rotation, offset and separation. The ratio can be obtained from equations (22) and (26b) as

$$K_r = \frac{\dot{D}_R}{\dot{D}} = \frac{2t\sec^2\phi + d\tan\phi}{2(d - 2t\tan\phi)}\tan\phi$$

or

$$K_r = \frac{G_r\sec^2\phi + \tan\phi}{2(1 - G_r\tan\phi)}\tan\phi, \quad (27)$$

where G_r is the ratio of width to length of layer-segments.

Equation (27) shows that the ratio K_r is a function of only two geometrical parameters G_r and ϕ. The curves for different K_r values in the co-ordinate system (ϕ, G_r) are shown in Fig. 7. It is evident that when $K_r \geq 1$ (e.g. for points above the solid line of Fig. 7) displacement of centres of the segments due to rotation in response to coupling forces exceeds or just equals the displacement of centres due to translation of layer-segments in response to the pulling force. As a result, layer-segments will show only rotation-and-offset without producing separation zones in between them. On the other hand, when $K_r < 1$ (e.g. for the points below the solid line of Fig. 7) the displacement of centres by translation of layer-segments exceeds the displacement by rotation of layer-segments, and separation zones will be produced along with rotation of layer-segments.

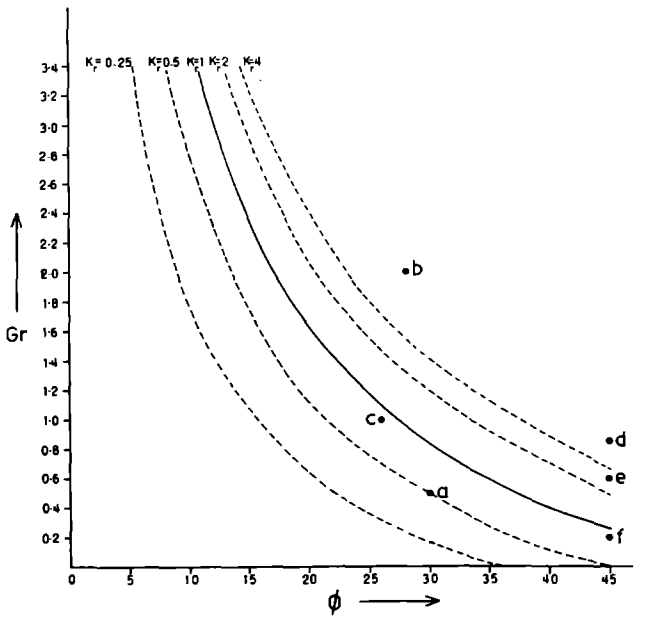

Fig. 7. Rate-curves for different K values; solid circles a, b, ... mark the experimental data.

DISCUSSION

The projection of geometrical data of the experiments in the co-ordinate frame (ϕ, G_r) reveals that those experiments (a, c and f) having ϕ G_r values below the theoretical curve $K_r = 1$ (Fig. 7) show development of separation zones along with rotation of layer-segments. On the other hand, those experiments (b, d and e) having values above the curve $K_r = 1$ show only rotation and offset of layer-segments without producing separation zones. So both the theory and the experiments concur that under layer-normal compression a rigid layer segmented by a set of parallel shear fractures may exhibit either separation or only rotation and offset of boudins depending upon their geometry. These results can be extended to natural deformed rocks where typical non-separated shear fracture boudins may grade to separated shear fracture boudins in a single competent layer due to decrease in the thickness to length ratio of boudins even though the orientation of fractures remain the same.

In the field $K_r < 1$ separation per unit rotation of layer-segments increases with the decrease in the K_r value. Such variation can be obtained by comparing experiments (a) and (c). Similarly, in the field $K_r > 1$ the increase of rate of rotation and offsetting of layer-segments with the increase in K_r value is observed in experiments (d) and (e).

In the present theoretical analysis the additional effect of flow-restriction due to rigid surface on the general stream function has been expressed by a simple exponential function which may not strictly hold in real situations. However, this does not matter on the applicability of equation (27) because the ratio of the two rates is considered here, and hence coefficients or other power-terms coming as constants with the differential form of the stream function will make no difference. On the same ground the coefficient of Y of the exponential

term in equation (20a) has been assumed to be unity. It is important to note that in the present theoretical consideration since the boundary conditions are given for the stage of initiation of movements in a segmented layer the equations will hold good up to a small amount of rotation of the layer-segments. However, this analysis may be extended to large movement of the layer-segments if the boundary conditions are modified at successive stages of a progressive deformation.

The positions of the curves in the field of ϕ and G_r are likely to be shifted when deformation is not of pure shear type. In this regard there may be some discrepancies if we attempt to fit a value obtained from natural deformed rocks with the theoretical curves presented here.

Acknowledgements—The authors are grateful to Professor S. K. Ghosh for his suggestions in developing the experimental set-up. They wish to thank Dr G. Mitra and two anonymous reviewers for upgrading the manuscript. They are also indebted to the Council of Scientific and Industrial Research, India, for providing the financial facilities.

REFERENCES

Cloos, E. 1947. Boudinage. *Trans. Am. geophys. Un.* **28**, 626–632.

Corin, F. 1932. Apropos du boudinage en Ardenne. *Soc. Belge. Geol.* **42**, 101–117.

Gay, N. C. & Jaeger, J. C. 1975. Cataclastic deformation of geological materials in matrices of different composition. II—Boudinage. *Tectonophysics* **27**, 323–339.

Griggs, D. T. & Handin, J. 1960. Observations on fracture and hypothesis of earthquake. In: *Rock Deformation* (edited by Griggs, D. T. & Handin, J.). *Mem. geol. Soc. Am.* **79**, 347–364.

Karmakar, S. & Mandal, N. 1989. Rotation and offset of shear fractures boudins. *Ind. J. Geol.* **61**, 41–49.

Lohest, M. 1909. Sur l'origine des veins et des geodes des terrains de Belgique. *Ann. Soc. géol. Belg.* **36**, 275–282.

Paterson, M. S. & Weiss, L. E. 1968. Folding and boudinage of quartz rich layer in experimentally deformed phyllite. *Bull. geol. Soc. Am.* **79**, 795–812.

Ramberg, H. 1955. Natural and experimental boudinage and pinch-and-swell structure. *J. Geol.* **63**, 512–526.

Ramsay, J. G. & Huber, M. I. 1983. *The Technique of Modern Structural Geology, Volume* 1: *Strain Analysis*. Academic Press, London.

Ramsay, J. G. & Huber, M. I. 1987. *The Technique of Modern Structural Geology, Volume* 2: *Folds and Fractures*. Academic Press, London.

Stach, E. 1982. *Coal Petrology* (3rd rev. and enlarged edn). Gebruder, Borntraeger, Berlin.

Tvergaard, V., Needleman, A. & Lo, K. K. 1981. Flow localization in the plane tensile test. *J. Mech. Phys. Solids* **29**, 115–142.

Uemura, T. 1965. Tectonic analysis of the boudin structure in the Muro Group, Ku Peninsula, Southwest Japan. *J. Earth Sci.* **13**, 99–114.

Wegmann, C. E. 1932. Note sur le boudinage. *Bull. Soc. géol. Fr.* 5 *Ser.* **11**, 477–489.